

Selection of Elevation Models for Flood Inundation Map Generation in Small Urban Stream: Case Study of Anyang Stream

Chanjin Jeong, Dong-Hyun Kim, Hyung-Ju Yoo, Seung-Oh Lee*

Department of Civil Environmental Engineering, Hongik University, Seoul, Korea

Received 15 April 2023; received in revised form 20 November 2023; accepted 21 November 2023

DOI: <https://doi.org/10.46604/aiti.2023.12000>

Abstract

To reduce flood damages, the Ministry of Environment in Korea has provided a flood inundation map so that people can expediently identify flood-prone areas. However, the current flood inundation maps have been produced based on the DEM which makes it difficult to represent realistic situations due to the lack of reproduction of land surface conditions. This study aims to provide more accurate and detailed flood inundation maps for flooding events due to river overflow in small urban areas. In this study, flood inundation analysis is performed using the river analysis system, HEC-RAS 2D, with the DSM and the DEM of urban areas in the Anyang Stream Basin, Korea to examine the differences in terms of terrain data and flooded area. Finally, for urban areas with dense buildings and congested road networks, the flood inundation analysis based on DSM can represent a more realistic flood situation and create an appropriate flood inundation map.

Keywords: urban flood inundation map, HEC-RAS 2D, DSM, DEM, terrain data

1. Introduction

Because of recent global climate change, damages due to droughts, floods, and typhoons have been increasing. This is because the energy cycle within the Earth is disrupted by global warming, causing greater differences in rainfall between regions. According to the World Meteorological Organization (WMO), climate-related disasters have caused 115 deaths per day on average over the past 50 years (1970-2019), and the number of disasters has increased fivefold during that period [1]. The Intergovernmental Panel on Climate Change's (IPCC) 6th assessment report predicts that regional variations in precipitation will continue to worsen due to climate change, and larger-scale floods will occur in the future [2].

As climate change worsens, defending against flood damage through structural measures is only a temporary solution [3]. Therefore, it is necessary to establish flexible flood defense measures that can adapt to the increasing extreme rainfall caused by climate change. As one of these measures, the city of Seoul identifies areas vulnerable to flooding by understanding the characteristics of the watershed and provides a flood inundation map that indicates areas expected to be flooded during extreme rainfall events. A flood inundation map is a map created by predicting areas that are likely to be flooded in advance to prevent human and property damage caused by floods due to extreme rainfall or levee break. Including Korea, many countries have produced a flood inundation map by predicting and analyzing the area and depth of flooding to effectively prevent flood damage. A flood inundation map should provide extensive information to mitigate flood damage and enable prompt preventive measures such as rapid evacuation of residents. They should also include basic data that can be effectively utilized for flood management [4].

* Corresponding author. E-mail address: seungoh.lee@hongik.ac.kr

However, the current flood inundation map only provides the expected flood range and depth, so the use of flood inundation maps is quite limited. It is difficult to obtain specific information because the expected flood range and depth are also provided quite roughly. In addition, using a digital elevation model (DEM) that does not consider facilities for flood analysis can lead to significant errors in densely populated urban areas [5]. There is a limit to citizens' active use of the current flood map because there may be significant errors. To achieve the actual purpose of production, which is flood control measures, it is necessary to develop a flood map.

Lee and Ha [6] simulated urban flooding using the US EPA stormwater management model (SWMM), hereafter referred to as XP-SWMM 2D. They analyzed changes in flood characteristics based on the presence or absence of buildings in the terrain data and argued that the reliability of the DEM decreases with the presence of buildings. The urban flooding in their study occurred due to poor drainage rather than river overflow. Lee et al. [7] also conducted flood simulations using HEC-RAS and developed flood inundation maps for a smaller area. Nevertheless, like the previous study, they interpolated the terrain construction using cross-sectional profiles of rivers, which resulted in flood maps that did not consider buildings on the land surface. Similarly, Salunke and Thube [8] simulated flooding in the Krishna basin, covering a large area of 55,537.60 km². They constructed terrain data with a resolution of 30 × 30 m using cross-sectional profiles of rivers and performed simulations using HEC-RAS. Due to the large-scale nature of the study area, the resolution of the terrain data had limitations, making it challenging to derive detailed results.

In this study, urban flooding due to river overflow in small urban areas is simulated. Unlike previous flood simulations in large areas, a suitable approach for small areas is adopted and more detailed results could be provided. HEC-RAS is used, and urban flooding was simulated due to river overflow, not poor drainage. Therefore, the purpose of this study is to produce a flood inundation map with a wider range of applications than current ones. For flood analysis in urban areas, HEC-RAS 2D, a two-dimensional numerical model, was selected, and the terrain data used for flood analysis was divided into DEM and digital surface model (DSM). The study analyzes variations in flood analysis outcomes attributed to disparities in terrain data and emphasizes the need for a flood inundation map that utilizes a DSM.

2. Methodology

The flowchart of this study is presented in Fig. 1. First, vulnerable areas to river flooding are selected by referring to the current flood inundation map. Secondly, a DSM is created using terrain data of the target area. Considering that the target area is a small-scale region, drone-based photogrammetry is performed as an economical and rapid method. Next, using HEC-HMS, scenarios of extreme rainfall are constructed according to frequency through hydrological analysis of the watershed, and flood inundation analysis is performed using HEC-RAS 2D with a focus on river flooding. Conducted a validation of the HEC-RAS 2D model through a comparison with the flood inundation maps using the FLUMEN model provided by the Ministry of Environment.

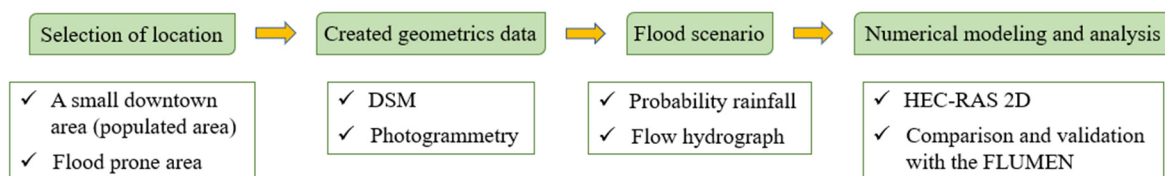


Fig. 1 Flowchart for generating a flood inundation map

3. Study Area

For this study, a small urban area within the Anyang Stream watershed in Seoul is selected as the target region. According to the River Master Plan [14], Anyang Stream is the first tributary of the Han River, with a watershed area of 283.75 km², a river length of 20.70 km, and a stream length of 33.33 km, based on the Anyang Stream estuary. The shape of

the watershed is dendritic and is located between $126^{\circ}52'37''$ to $126^{\circ}54'54''$ east longitude and $37^{\circ}24'35''$ to $37^{\circ}33'14''$ north latitude. Due to the geographical characteristics of the Anyang Stream watershed located in the Seoul metropolitan area, most of the lower parts of the watershed are urban areas, and various factories and public facilities are scattered throughout the watershed.

As shown in Fig. 2, the target area includes the stream and floodplain from Ogum Bridge to Gochuk Bridge in the Anyang Stream watershed. Although it is a small area with a length of 1km and an area of 0.4 km^2 , it is characterized by a high concentration of industrial facilities and residential areas. Currently, it is legally restricted to take pictures using drones for personal reasons in Korea. Therefore, when performing flood simulation, this study only targeted small areas that could show the difference between DEM and DSM. According to the current flood inundation map, the area is predicted to be flooded with a depth of more than 2 m in the event of a flood, requiring a prompt response from residents.

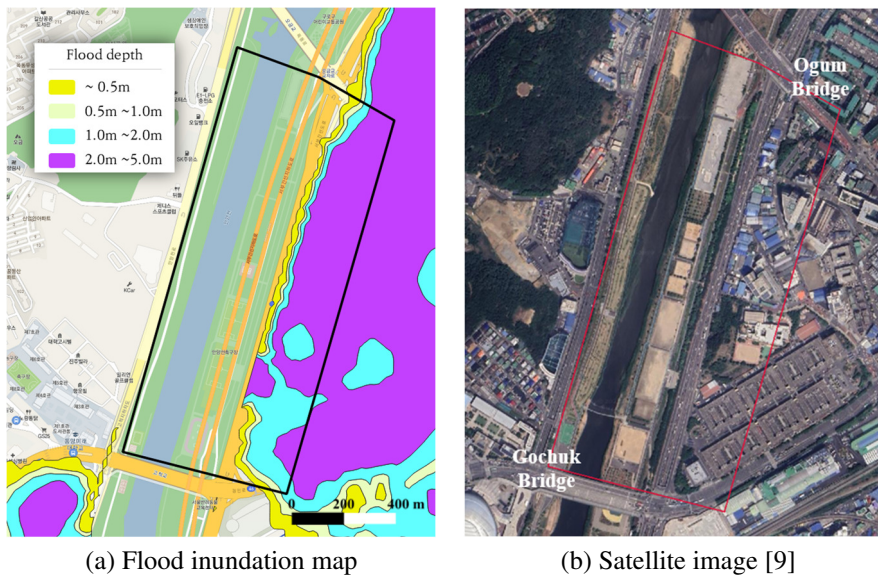


Fig. 2 Flood inundation in the study area [9]

4. Terrain Survey

A flood inundation map is used to identify areas that are likely to be flooded during a given flood event. This map is typically created using hydraulic models that simulate water flow based on terrain data. That is why terrain data plays a crucial role in accurate flood analysis. The terrain data used for flood analysis can be broadly divided into two types: DEM and DSM. Fig. 3 shows the difference between DSM and DEM [10].

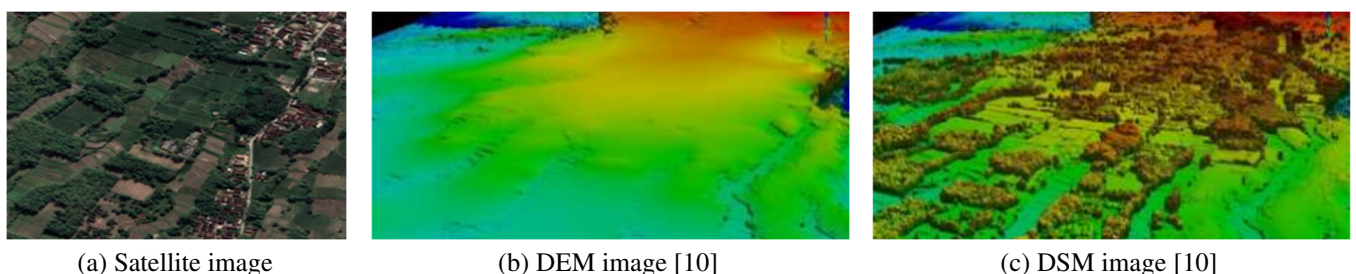


Fig. 3 Comparison of DEM and DSM

The DEM is terrain data indicating the height of the ground surface by excluding height information of buildings or vegetation. While the DSM can provide detailed information about the height and location of all objects on the Earth's surface, including buildings and vegetation, but may not accurately represent the actual ground level. The DSM can lead to an overestimation of flood depth and extent because it contains information not only on buildings but also on objects that

interfere with flood analysis. For this reason, DEM is currently preferred over DSM for flood inundation mapping. However, with the recent development of surveying technology, DSM construction technology using LiDAR or drone technology has been developed. This can economically generate higher quality and accurate topographic data than before [11], so it is necessary to review flooding analysis based on DSM.

4.1. Drone and camera properties

In this study, the DJI Mini 2 drone is utilized for aerial photography to facilitate the application of photogrammetric techniques. The Mini 2 drone, manufactured by DJI, is known for its lightweight design, weighing only 249 g, which enhances its ease of use during fieldwork. Its camera supports up to 4k resolution, allowing for high-resolution photo capture and providing the foundational data for accurate terrain modeling. The detailed specifications of the drone and camera are provided in Table 1. The drone has an automatic flight mode that can be controlled using a smartphone, making it possible to plan and execute systematic flight paths, adjust flight speed and altitude, and set shooting overlaps [12].

Table 1 Drone and camera specification

Classification		Contents
Drone	Size	245 × 289 × 56 mm
	Weight	249 g
	Battery	2250 mAh
	Flight time	31 minutes
	Flying speed	16 m/s
Camera	Focal length	4.7 mm
	Sensor	1/2.3" CMOS
	Data format	JPEG, DNG
	Image size	4000 × 3000
	FOV	83°

4.2. Photogrammetry

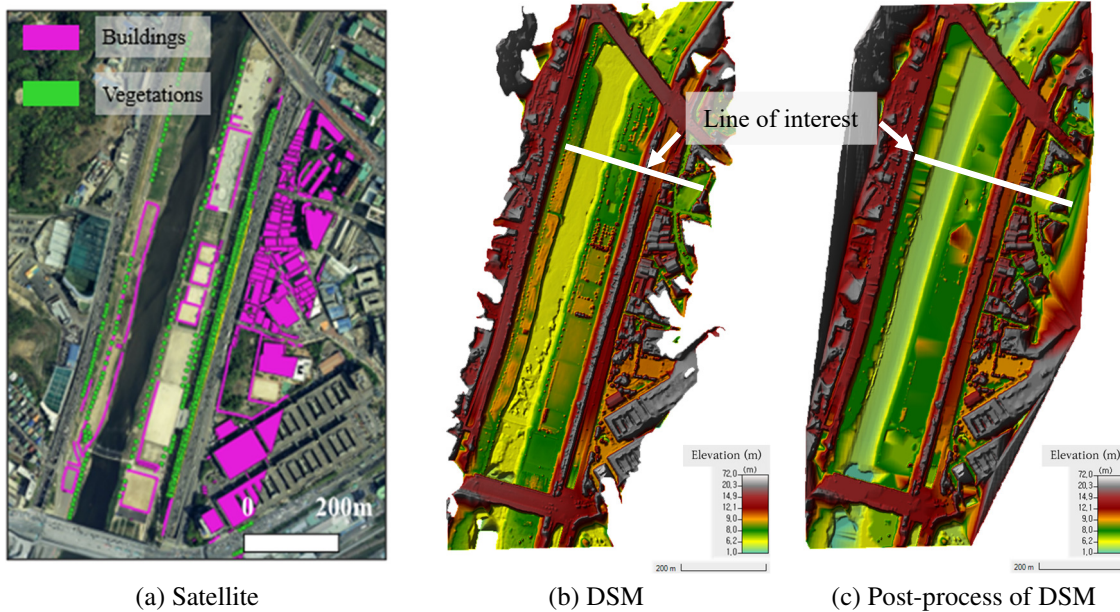


Fig. 4 DSM of the study area

In this study, a drone-based photogrammetric method is selected to construct a DSM for a small urban area. Drones enable rapid and accurate collection of geospatial information in small areas, but using lightweight drones for aerial photography can result in increased instability due to wind. To maintain high precision of terrain data, images are captured with approximately 70% vertical and horizontal overlap at a low altitude [12]. This required a large number of photos, and a

total of 1415 images are captured. High-resolution photos were then used to generate a 2 m resolution DSM using Bentley's Context Capture software. A comparison of the DSM with satellite imagery of the target river shows that the features identified in the satellite imagery were similar to those in the DSM.

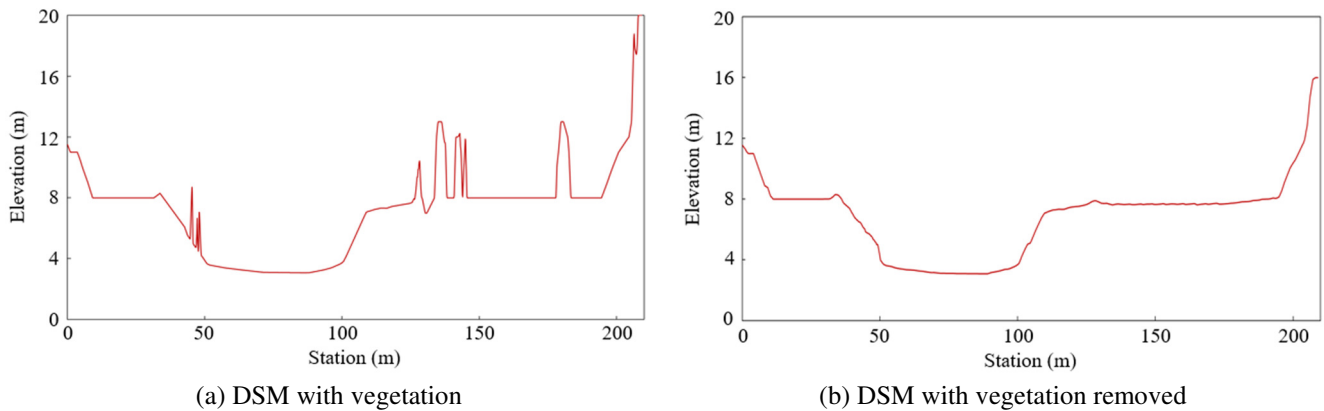


Fig. 5 Cross-section of the line of interest (LOI)

The results of constructing a DSM through photogrammetry revealed the presence of vegetation information that could act as an error factor in flood analysis. In the case of flood analysis, vegetation information can have an inaccurate impact on water flow. Therefore, vegetation data were removed using filtering. Additionally, in photogrammetry, the height of the channel is inaccurate due to light reflection and the flow of water in the river. Thus, the river's channel in the DSM was adjusted, along with cross-sections based on actual measurements. As shown in the cross-sectional view in Figs. 4 to 5, unnecessary information for flood analysis was removed. Since the DSM includes information on all objects above the surface, post-processing to modify terrain information is essential.

4.3. Conversion DSM to DEM

The method of converting DSM to DEM is to remove the information about obstacles, such as buildings, from the DSM. The study utilized the building information of the target region to filter out and eliminate the building information. Subsequently, a smoothing process was executed to develop a more precise DEM. The result is shown in Fig. 6.

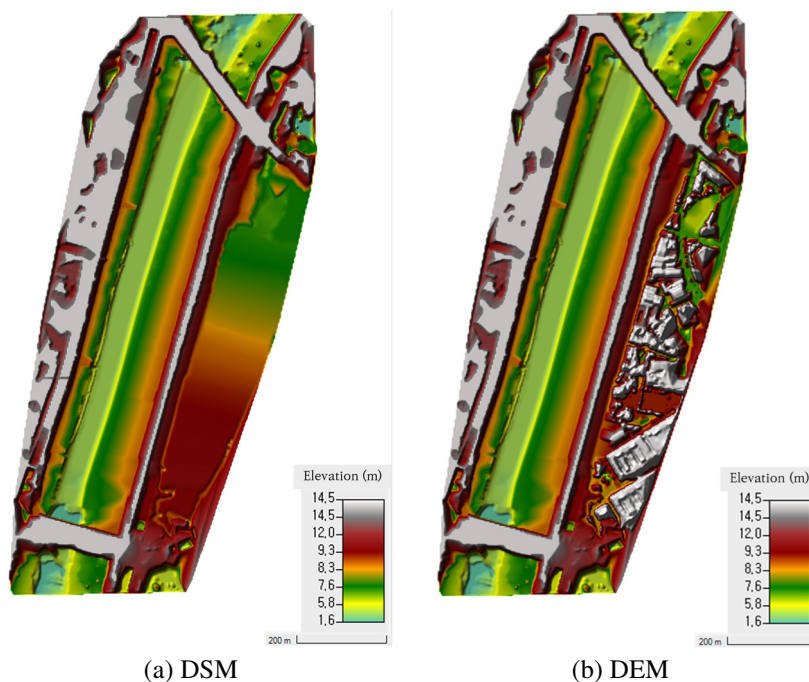


Fig. 6 Conversion of DSM to DEM

5. HEC-HMS Model

HEC-HMS is a hydrologic modeling software developed by the U.S. Army Corps of Engineers Hydrologic Engineering Center (HEC). The software simulates and analyzes the hydrologic response of watersheds to various precipitation. HEC-HMS allows users to define the physical characteristics of a watershed, including land use, soil types, and topography, and to specify various precipitation inputs, such as rain or snowfall. The software uses this information to calculate the resulting hydrographs, which can be used to analyze the behavior of streams, rivers, and other bodies of water [13].

Table 2 Basin characteristic of Anyang Stream, Korea

River	Area (km ²)	Time of concentration (hr)	Storage coefficient (hr)	Curve number
Anyang Stream	211.25	4.47	3.78	87.9

In this study, the probability of rainfall maximum precipitation is calculated using rainfall data from Seoul and Suwon weather observation stations until 2021, considering the study area. The flood discharge is calculated using Clark's unit hydrograph method. Clark's unit hydrograph method can synthesize a unit hydrograph using the time of concentration and the storage coefficient of the watershed, and its consistency and objectivity have been proven. In addition, the watershed characteristics that must be entered in the HEC-HMS, such as area, curve number, and concentration time as shown in Table 2, are referenced in the River Master Plan [14]. All hydrograph scenarios used are constructed through frequency analysis in HEC-HMS. Through HEC-HMS, four flow hydrographs, as shown in Fig. 7, are being derived. The peak flow gradually increases from the 50-year frequency rainfall to the 500-year frequency rainfall, and the peak flow for each scenario increases from 1735 m³/s to 2423 m³/s.

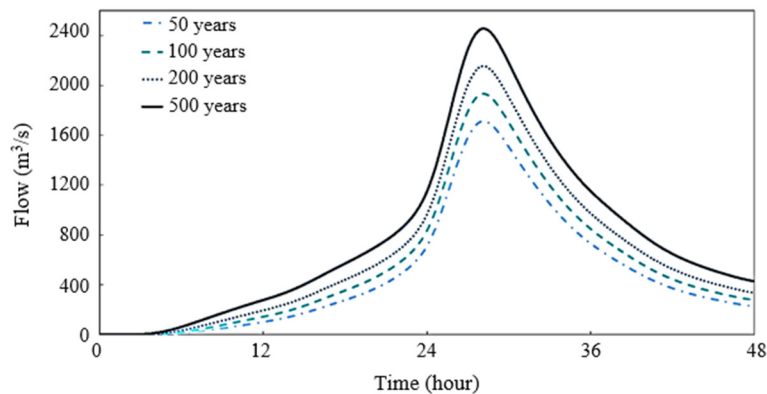


Fig. 7 Flow hydrograph scenarios for various return periods

6. HEC-RAS 2D Model

HEC-RAS 2D is a hydraulic model developed by the U.S. Army Corps of Engineers and is an extended system of the HEC-2 model that analyzes the water surface curve. HEC-RAS 2D is open-source software and is widely used for hydraulic modeling because it is a program that does not require a license. The HEC-RAS 2D model can simulate the effects of the sediment transport model, water temperature model, bridge excavation calculation, and hydraulic structure on both steady and unsteady flows. In addition, it can analyze and express the effects of flooding of floodplains and levees in two dimensions. This study performed a two-dimensional simulation using HEC-RAS 2D, and it can calculate the flood depth, water surface elevation, and velocity using multiple polygonal grids.

6.1. Governing equations in HEC-RAS 2D

HEC-RAS 2D can efficiently and stably perform two-dimensional simulations using either the Saint-Venant equations or the diffusion wave equations. The time step for running the model is determined by the formula associated with the Saint-Venant equation (full momentum), ensuring quick and stable simulations [15]:

$$C = \frac{V\Delta T}{\Delta X} \leq 1.0 \text{ (with a max } C = 3.0) \quad (1)$$

$$C = \frac{V\Delta T}{\Delta X} \leq 2.0 \text{ (with a max } C = 5.0) \quad (2)$$

where C is the Courant number, V is flood wave celerity, ΔT is the computational time step and ΔX is the average cell size.

In the case of simulating 2D unsteady flow, the calculation is performed according to the equations of mass conservation:

$$\frac{\partial h}{\partial t} + \frac{\partial(hu)}{\partial x} + \frac{\partial(hv)}{\partial y} = q \quad (3)$$

and momentum conservation:

$$\frac{\partial u}{\partial t} + \frac{u\partial u}{\partial x} + \frac{v\partial u}{\partial y} - f_c v = -g \frac{\partial z_s}{\partial x} + v_t \left(\frac{\partial^2 u}{\partial x^2} + \frac{\partial^2 v}{\partial y^2} \right) - \frac{\tau_{b,x}}{\rho R} + \frac{\tau_{s,x}}{\rho h} \quad (4)$$

$$\frac{\partial v}{\partial t} + \frac{u\partial v}{\partial x} + \frac{v\partial v}{\partial y} - f_c u = -g \frac{\partial z_s}{\partial y} + v_t \left(\frac{\partial^2 v}{\partial x^2} + \frac{\partial^2 v}{\partial y^2} \right) - \frac{\tau_{b,y}}{\rho R} + \frac{\tau_{s,y}}{\rho h} \quad (5)$$

where t is time, u is the velocity component in the x -direction, v is the velocity component in the y -direction, z_s is water surface elevation, h is the water depth, q is a source/sink flux term, f_c is the Coriolis parameter, g is gravitational acceleration, v_t is horizontal eddy velocity, τ_b is bottom shear stress, τ_s is the surface wind stress, and R is the hydraulic radius.

6.2. Model validation

In this paper, numerical modeling using HEC-RAS was conducted, encompassing both channel and interior floodplain. To verify the reliability of the HEC-RAS model employed in the study, validation processes are conducted separately for the channel and interior floodplain, thereby demonstrating the suitability of the HEC-RAS model.

(1) Channel

To verify the HEC-RAS 2D model for the channel, a comparison is performed with the water surface elevation observed in the study area. The water surface elevation data of June 15, 2009, at three points between Ogum Bridge and Gochuk Bridge presented in the Anyang River Master Plan [14] were compared with the water surface elevation data calculated by the HEC-RAS 2D simulation. As shown in Table 3, the water surface elevation observed at three stations was compared with the water surface elevation calculated by the HEC-RAS 2D model, and the average error was about 2.5%.

Table 3 Error of water surface elevation calculated by HEC-RAS 2D

Station	Observed (m)	HEC-RAS 2D (m)	Error (%)
6 + 239	4.12	4.23	2.67
6 + 487	4.19	4.31	2.86
6 + 733	4.32	4.41	2.03

(2) Interior floodplain

The Ministry of Environment provides the public with a flood inundation map calculated by FLUMEN, and in this study, it could be used as verification data for the HEC-RAS 2D model. Since there is no actual flood area in the study area, it had to be compared with the flood inundation map calculated by FLUMEN, a two-dimensional hydraulic model. In this study, the two-dimensional hydraulic model is verified by calculating the goodness of fit [16] between the flood area shown

in the flood inundation map and the flood area calculated by HEC-RAS 2D. To apply the same conditions as the flood inundation map, the DSM is edited into DEM. In addition, the levee break scenario is applied, and the 100-year frequency flood is input as the boundary condition of the model.

$$Fit(\%) = \frac{A_{FLUMEN} \cap A_{HEC-RAS\ 2D}}{A_{FLUMEN} \cup A_{HEC-RAS\ 2D}} \times 100 \tag{6}$$

where $Fit(\%)$ is the model goodness of fit percentage, A_{FLUMEN} is the flood area shown in the flood inundation map, and $A_{HEC-RAS\ 2D}$ is flood area calculated by HEC-RAS 2D.

To analyze the goodness of fit, each flood area is calculated based on the 2.0 m to 5.0 m area of the flood inundation map. The flood area (A_{FLUMEN}) shown in the flood inundation map was 0.079 km², and the flood area ($A_{HEC-RAS\ 2D}$) calculated by HEC-RAS 2D was 0.091 km². Each area is shown in Fig. 8. When the two areas are compared, it was confirmed that the spatial distribution of the flood area showed a similar shape. As a result of these results, a fit of about 70% could be obtained by applying Eq. (6).

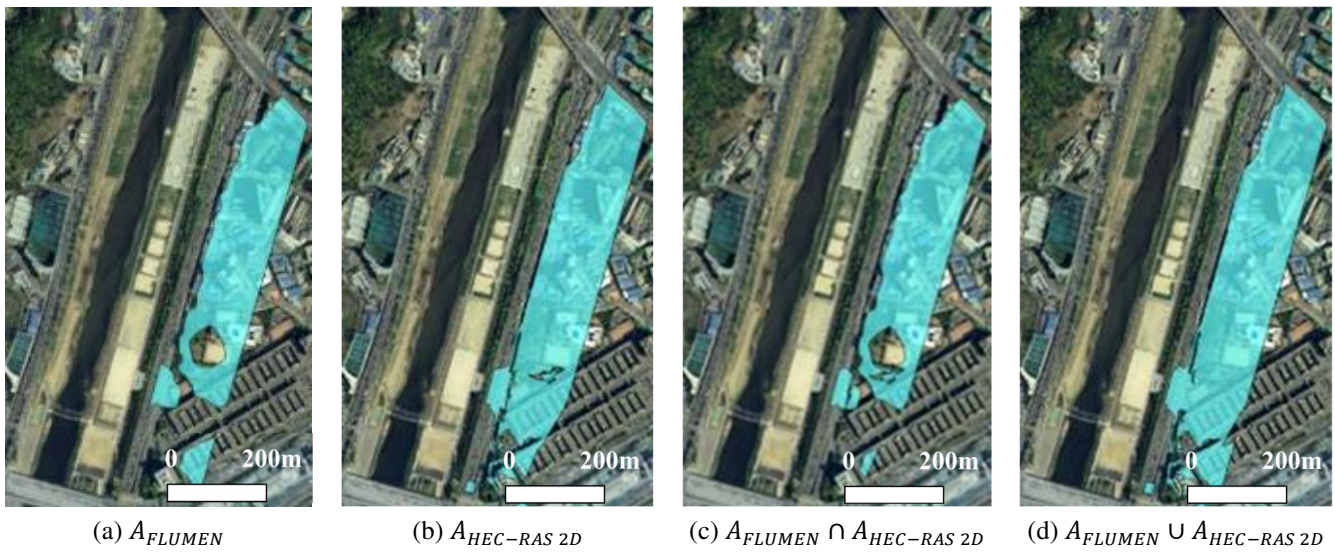


Fig. 8 Model validation between FLUMEN and HEC-RAS 2D using DEM

6.3. Parameters for simulation

Table 4 Numerical modeling parameters in HEC-RAS 2D

Flow area	0.4 km ²
$\Delta x, \Delta y$ size	2 m \times 2 m
Grid number	Total: 91594
Manning's n values	Channel: 0.027 Floodplain: 0.030 Interior floodplain: 0.020
Boundary condition	Upstream: flow hydrograph (scenario) Downstream: normal depth (1/2369) Interior floodplain: outflow
Computation time step	1 second

The flood area is calculated from Gochuk Bridge (upstream) to Ogeum Bridge (downstream), including the right interior floodplain. To obtain stable simulation results, parameters such as grid size and calculation time are set to ensure that the Courant number did not exceed 2. The grid size is set to an average of 2 m and the time step was set to 1 second. The Manning's n values are input based on the River Master Plan [14]. The boundary conditions consisted of flow hydrograph upstream, normal depth downstream, and outflow at the land boundary conditions. Table 4 provides detailed variables for the HEC-RAS 2D simulation.

7. Results

The results obtained from the numerical model HEC-RAS in this study are as follows: The outcomes of the HEC-RAS model allowed for an intuitive and quantitative understanding of the difference between DEM and DSM. After analyzing the simulation results based on two terrain data, an economic feasibility study was conducted.

7.1. HEC-RAS 2D results and analysis by terrain data

When simulating rainfall scenarios of 50-year, 100-year, and 200-year frequency using HEC-RAS 2D for flood analysis, no flooding occurred up to the interior floodplain. However, when simulating the rainfall scenario of 500-year frequency, the river overflowed and caused flooding up to the project boundary. In the 500-year frequency rainfall scenario, flooding began in the project boundary and reached its maximum depth within two hours. The following Figs. 9-11 show the results obtained using DEM and DSM, respectively, in the 500-year rainfall frequency scenario.

The difference in simulation results based on DEM and DSM can be seen from the Figs. 9-11. DEM, which is based on terrain data without considering structures, could not accurately predict the exact depth and velocity for each location. However, DSM, which considers the flow between buildings, could express the effect of buildings on flooding. The water surface elevation calculated from the DEM-based flood analysis was 13.35 m, while that from the DSM-based analysis was 14.48 m. A difference of over 1.0 m in flood level was observed, which was due to the occupancy area of the buildings. Based on the current analysis, buildings are not shown as inundation areas on the map. It means that the flood depth is not higher than the buildings, and if the flood depth becomes higher than the buildings, the area where the buildings are located will also appear as an inundation area.

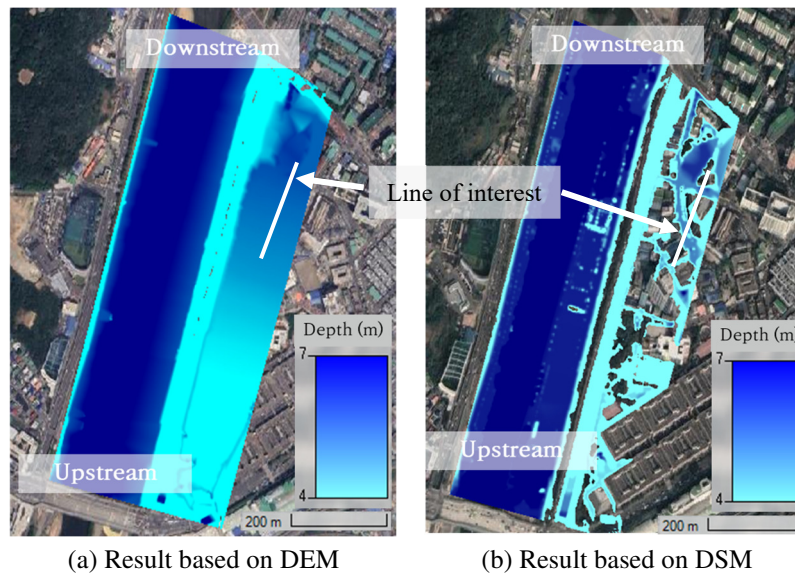


Fig. 9 Results of depth in 500-year frequency rainfall scenario

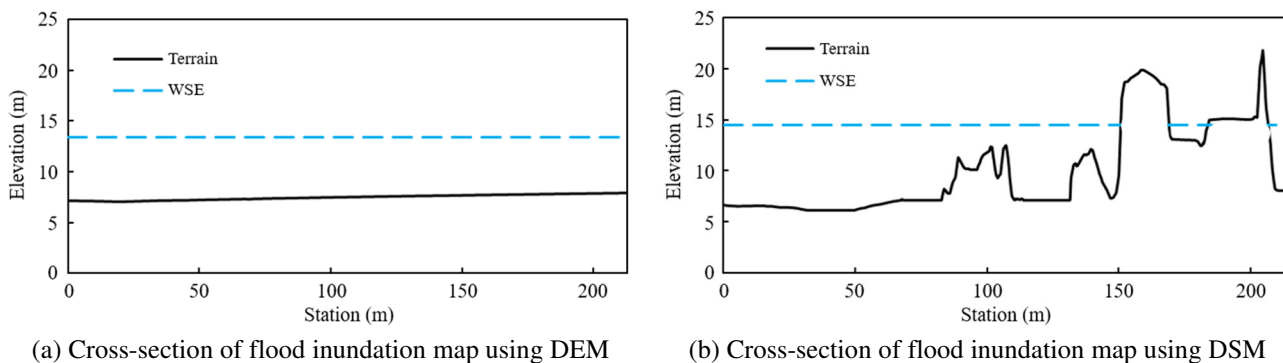


Fig. 10 Cross section of the line of interest

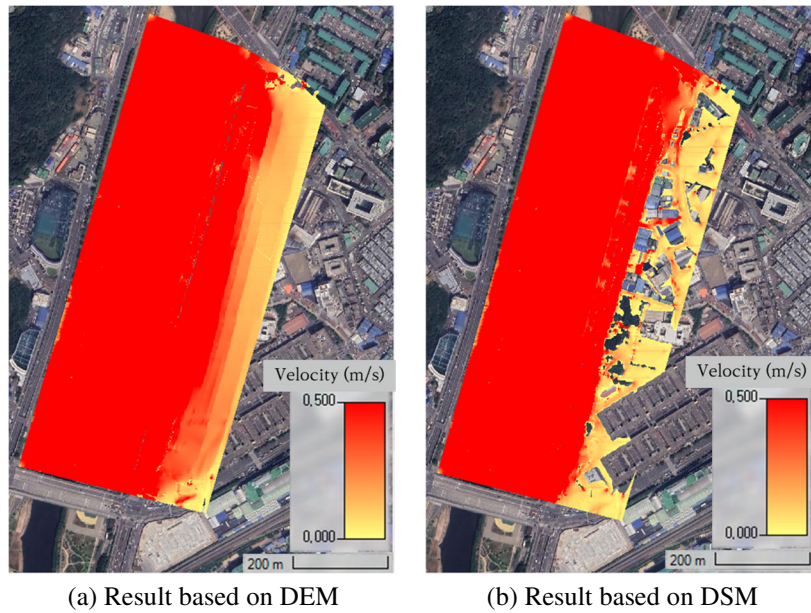
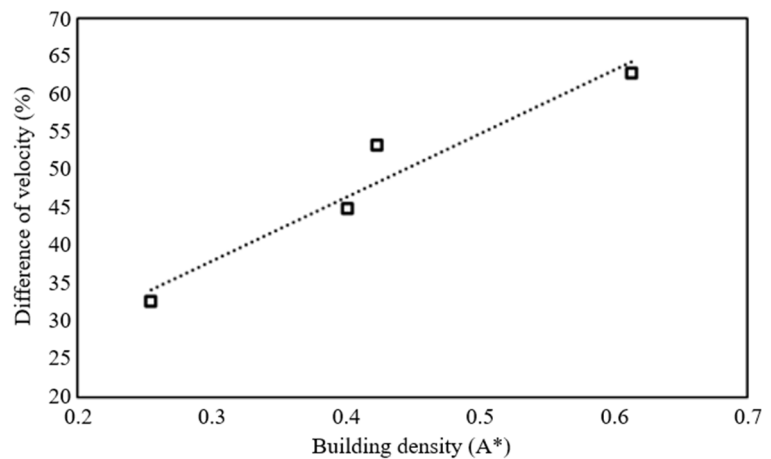


Fig. 11 Results of velocity in 500-year frequency rainfall scenario

The velocity showed a higher value when based on DSM, but it cannot be considered accurate and detailed as it does not consider the influence of buildings. However, in the DSM-based results, the velocity near the buildings is higher than in other areas. As depicted in Fig. 12, variations in velocity were observed to be different based on building density (the proportion of the total area of a section occupied by buildings) when comparing the velocities obtained from DEM and those obtained from DSM. When buildings occupied approximately 25% of the area, a difference of around 30% in velocity was noted compared to DEM. Conversely, in areas where buildings covered approximately 60% of the region, a velocity difference of approximately 60% was observed.



(a) Building density by section



(b) Difference in velocity between DEM and DSM according to building density ($A^* = A_{Building}/A_{Total}$)

Fig. 12 Difference in velocity on roads based on building density in different sections

Generally, an increase in velocity is observed in proportion to the extent of building coverage. This phenomenon is particularly pronounced in densely populated urban areas, where the differences between velocities in DEM and DSM are substantial. Therefore, it is advisable to consider an increase in velocity corresponding to building density when interpreting velocity results obtained from DEM.

7.2. Korean-flood risk assessment model [17]

Korean-flood risk management (K-FRM) is an assessment technique that quantitatively presents flood risk applied in Korea. These results present variations in flood risk assessment when using flood inundation maps derived from both DSM and DEM terrain data. Currently, flood risk assessment has been conducted using flood inundation maps created from DEM terrain data. However, by utilizing flood inundation maps based on DSM terrain data, the results of flood risk assessment exhibit significant differences.

Economic losses from natural disasters are the financial impact of unforeseen disasters from an economic point of view, and these losses require several steps: risk analysis for disaster guidance, asset list for disaster space distribution and scale, damage function definition, and eventually loss quantification. K-FRM considers various types of flood damage, including building damage, vehicle damage, agricultural damage, human casualties, and public facilities damage, which are tailored to specific conditions in South Korea and may vary depending on region and type of disaster. The K-FRM follows a scheme as shown in the following figure.

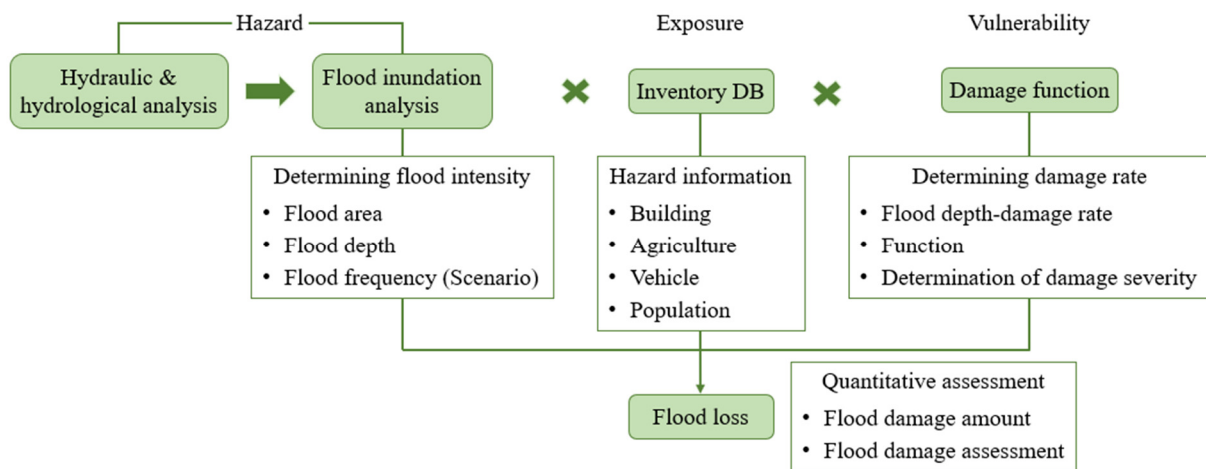


Fig. 13 Flood damage analysis framework in K-FRM [17]

Following the K-FRM methodology, flood damage amounts are determined based on flood inundation maps. Therefore, in this study, flood damage in the research area is assessed using flood inundation maps generated from DSM. The results reveal that the flood damage amount based on DEM is approximately 24% higher than that calculated using DSM. This suggests the potential risk of overestimating flood damage when utilizing DEM terrain data, thereby providing a rationale for employing it in the creation of flood inundation maps.

Table 5 Difference in flood damage assessment amount between DEM and DSM (Unit: USD 1,000)

Terrain data	Vehicle	Life	Victim	Crops	Farmland	Sum
DEM	12,175.66	95.55	56.44	0.45	2.81	12330.91
DSM	9944.35	85.86	51.12	0.45	2.80	9944.35

7.3. Flood inundation map

A flood inundation map is created using the results of flood analysis based on DSM. The flood inundation map shows a clear difference from the current flood inundation map based on the DEM. In addition, by conducting HEC-RAS 2D simulations, flood depths, flood extent, and velocities over time can be derived. Therefore, it is possible to predict the flood situation in the flood inundation map over time. It can be observed that the flood progresses from both ends to the center.

As shown in Figs. 14-15, it can be seen that it takes only one hour from the start of flooding until the entire area is completely inundated. When fully inundated, the depth of flooding exceeds 4 m, and the velocity is close to 0.5 m/s. An important point to note is that the flood depth and velocity have different values depending on the distribution. U.S.

Department of the Interior [18] provided details of the classification of the hazard ratio. Under this classification, if the depth of the flood is more than 1.5 m and the flow rate is more than 0.5 m/s, it belongs to the high-danger zone, and it is assumed that lives are in jeopardy. In the scenario of this study, the area to be studied belongs to the high-danger zone, and residents need to respond in advance from flooding.

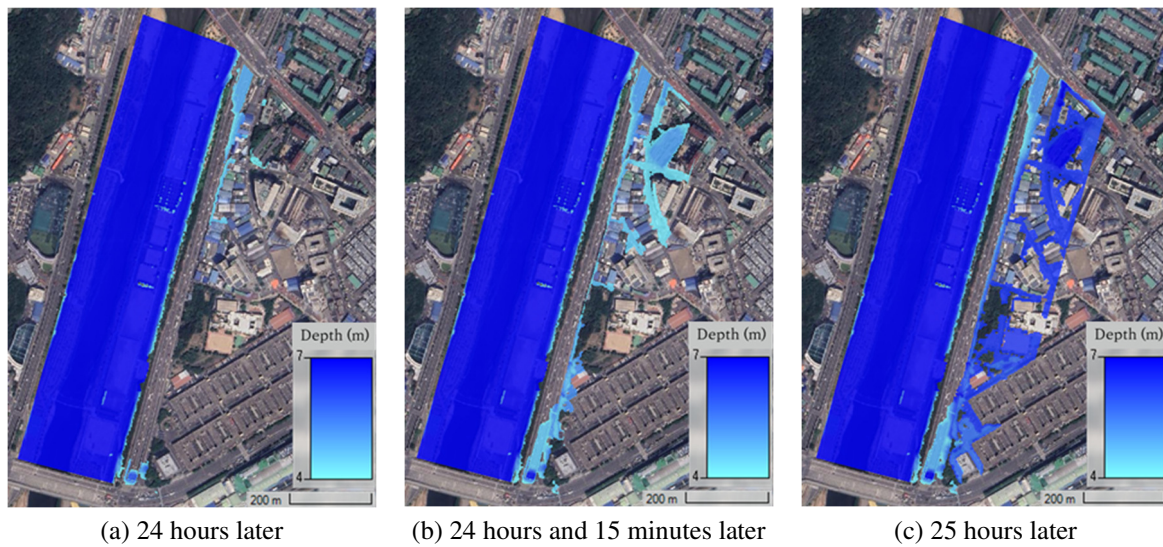


Fig. 14 Flood inundation map for depth and extent of flooding by duration

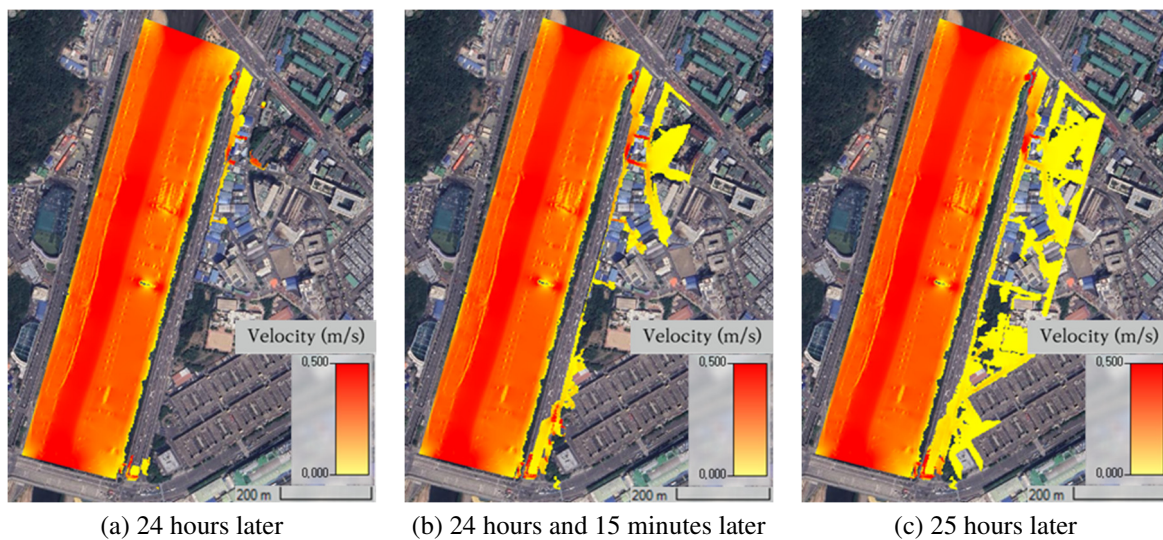


Fig. 15 Flood inundation map for the velocity of flooding by duration

8. Conclusion

In this study, differences in flood inundation analysis results for urban areas based on DEM and DSM using the HEC-RAS 2D model were confirmed through hydraulic and economic feasibility analysis. Conducting flood inundation analysis by removing all building information in a continuously developing city would no longer be considered a meaningful endeavor. Unlike the current flood inundation map calculated with DEM, the flood inundation map generated with DSM provides additional information such as velocities and paths for sequential time steps. The most significant distinction between flood inundation maps based on DEM and DSM lies in the realism of the flood inundation map.

Since DSM represents terrain information that closely resembles the actual topography compared to DEM, conducting flood analysis based on DSM enables us to create a more realistic flood inundation map. Accurate flood inundation analysis using DEM data in densely urbanized areas with numerous buildings and infrastructure is challenging. As Seoul, Korea,

continues to experience rapid urbanization and expansion, employing DSM for flood inundation analysis may be a suitable approach for detailed evacuation and defense planning. Furthermore, this study used its findings to calculate flood damage, advocating that the creation of flood inundation maps using DSM is appropriate. The assertion is not solely based on the differences in direct information, such as depth and velocity, between flood inundation maps generated from DSM and DEM. Instead, it stems from the evaluation of the suitability of DSM for producing flood inundation maps from the perspective of flood damage estimation.

In this study, the simulation of river flooding was focused on the small-scale urban area. However, to simulate larger areas encompassing inland regions, both river flooding and inland inundation analysis should be conducted. Moreover, the need for inland inundation analysis is increasing due to frequent incidents of inland flooding, often attributed to urban drainage systems being unable to handle recent extreme rainfall events. In the future, it will be essential to create more accurate flood inundation maps using DSMs that simultaneously consider both river inundation and inland flooding in urban areas.

Acknowledgment

This research was supported by a grant (2022-MOIS61-005 (RS-2022-ND634032)) for the Development of Risk Prediction Technology for Storms and Floods for Climate Change based on Artificial Intelligence, funded by the Ministry of Interior and Safety (MOIS, Korea)

Conflicts of Interest

The authors declare no conflict of interest.

References

- [1] World Meteorological Organization (WMO), WMO Bulletin, vol. 71, no. 1, Switzerland: WMO, 2022.
- [2] T. Kanitkar, A. Mythri, and T. Jayaraman, "Equity Assessment of Global Mitigation Pathways in the IPCC Sixth Assessment Report," unpublished.
- [3] E. E. Koks, K. C. H. van Ginkel, M. J. E. van Marle, and A. Lemnitzer, "Brief Communication: Critical Infrastructure Impacts of the 2021 Mid-July Western European Flood Event," *Natural Hazards and Earth System Sciences*, vol. 22, no. 12, pp. 3831-3838, November 2022.
- [4] I. H. Son, "Flood Risk Map Overseas Production Case," *Water for Future*, vol. 45, no. 9, pp. 99-105, 2012. (In Korean)
- [5] S. U. Kim, K. W. Jun, S. H. Lee, and W. S. Pi, "Analysis of the Impact of Building Congested Area for Urban Flood Analysis," *Journal of Korean Society of Disaster and Security*, vol. 15, no. 3, pp. 41-46, September 2022.
- [6] J. Y. Lee and S. R. Ha, "Impact of Building Blocks on Inundation Level in Urban Drainage Area," *Journal of Environmental Impact Assessment*, vol. 22, no. 1, pp. 99-107, 2013.
- [7] D. H. Lee, K. W. Jun, and I. D. Kim, "A Study on the Production of Flooding Maps in Small Stream," *Journal of Korean Society of Disaster and Security*, vol. 14, no. 2, pp. 51-59, June 2021.
- [8] S. Salunke and A. D. Thube, "Floodplain Mapping of Krishna River at Karad Using HEC-RAS," *International Research Journal of Engineering and Technology*, vol. 9, no. 7, pp. 1444-1450, July 2022
- [9] "Ogeumgyo - Google Maps," <https://maps.app.goo.gl/bExCumDsTsX7ngJYA>, January 10, 2023.
- [10] J. Wang, L. Wang, M. Jia, Z. He, and L. Bi, "Construction and Optimization Method of the Open-Pit Mine DEM Based on the Oblique Photogrammetry Generated DSM," *Measurement*, vol. 152, article no. 107322, February 2020.
- [11] N. H. Pandjaitan, Sutoyo, M. I. Rau, J. Febrita, I. Dharmawan, and I. Akhmat, "Comparison between DSM and DTM from Photogrammetric UAV in Ngantru Hemlet, Sekaran Village, Bojonegoro East Java," *Proceedings of SPIE, Sixth International Symposium on LAPAN-IPB Satellite*, vol. 11372, article no. 113723, 2019.
- [12] J. H. Yoon and G. H. Kim, "3D Building Mapping using Drone," *Korean Society of Surveying, Geodesy, Photogrammetry, and Cartography*, pp. 101-102, 2020. (In Korean)
- [13] D. Halwatura and M. M. M. Najim, "Application of the HEC-HMS Model for Runoff Simulation in a Tropical Catchment," *Environmental Modelling & Software*, vol. 46, pp. 155-162, August 2013.

- [14] Ministry of Land, Infrastructure and Transport, “Anyang River Master Plan,” Construction Technology Digital Library, Technical Report OTKCRK200735, December 2015. (In Korean)
- [15] E. Ghimire, S. Sharma, and N. Lamichhane, “Evaluation of One-Dimensional and Two-Dimensional HEC-RAS Models to Predict Flood Travel Time and Inundation Area for Flood Warning System,” *ISH Journal of Hydraulic Engineering*, vol. 28, no. 1, pp. 110-126, 2022.
- [16] S. H. Lee, D. S. Lee, J. M. Kim, and B. S. Kim, “Study on 2-D Urban Flood Inundation Analysis Using Digital Surface Model (DSM) and Digital Elevation Model (DEM),” *KSCE Journal of Civil and Environmental Engineering Research*, pp. 351-352, 2016. (In Korean)
- [17] G. H. Kim and G. T. Kim, “Development of Flood Damage Estimation Model (K-FRM) Analysis Tool to Support Economy Analysis,” *Water for Future*, vol. 54, no. 5, pp. 14-22, 2021. (In Korean)
- [18] D. J. Trieste and U. S. Bureau of Reclamation, “Downstream Hazard Classification Guidelines,” Denver: U.S. Department of the Interior Bureau of Reclamation, 1988.



Copyright© by the authors. Licensee TAETI, Taiwan. This article is an open-access article distributed under the terms and conditions of the Creative Commons Attribution (CC BY-NC) license (<https://creativecommons.org/licenses/by-nc/4.0/>).